Symplectic integrators: An introduction

Denis DonnellyEdwin Rogers

Citation: American Journal of Physics **73**, 938 (2005); doi: 10.1119/1.2034523
View online: http://dx.doi.org/10.1119/1.2034523
View Table of Contents: http://aapt.scitation.org/toc/ajp/73/10
Published by the American Association of Physics Teachers

Symplectic integrators: An introduction

Denis Donnelly[a)]
Department of Physics, Siena College, Loudonville, New York 12211

Edwin Rogers[b)]
Department of Mathematics, Siena College, Loudonville, New York 12211

(Received 26 February 2004; accepted 21 July 2005)

Symplectic integrators very nearly conserve the total energy and are particularly useful when treating long times. We demonstrate some of the properties of these integrators by exploring the structure of first-, second-, and fourth-order symplectic integrators and apply them to the simple harmonic oscillator. We consider numeric, geometric, and analytic aspects of the integrators with particular attention to the computed energies. © *2005 American Association of Physics Teachers.*
[DOI: 10.1119/1.2034523]

I. INTRODUCTION

It is frequently necessary to follow the evolution of a dynamical system by means of a numerical integration for long times. In this case, if the system is described by a time-independent Hamiltonian, symplectic integration methods can be superior to general purpose ordinary differential equation solvers. For example, Runge-Kutta methods do not conserve the total energy. If we apply the fourth-order fixed step Runge-Kutta method to the simple harmonic oscillator, the computed energy value drifts from the true value and the results are surprisingly poor. These results are dramatically improved using an adaptive step size, but this method is computationally more costly and the computed energy continues to drift from the true energy, albeit more slowly. In this paper, we introduce several simple symplectic algorithms and show that these algorithms do not exhibit this problem.

Symplectic methods belong to the larger class of geometric numerical integration algorithms. These algorithms are constructed so that they preserve certain geometrical properties inherent in the system. Symplectic methods are so named because, when applied to problems in Hamiltonian mechanics, the algorithms preserve the linear symplectic structure inherent in the phase space representation of the dynamics. The first of these methods was developed by de Vogelaere.[1] These methods were later developed independently by Ruth,[2] who constructed symplectic integrators while investigating the dynamics of particle accelerators. Since then, symplectic algorithms have been employed in fields such as molecular dynamics and astronomy.[3–12] Early on, it was observed that for such methods, the error in the energy remains bounded over significant times (see, for example, Ref. 7). This fact, and the relative simplicity of the algorithms, initiated further development of symplectic methods and their applications.

In this article, we introduce simple first-, second-, and fourth-order symplectic integrators and examine their structure for the simple harmonic oscillator from a numerical, geometric, and analytic standpoint. The advantage of this one-dimensional example is that the dynamics associated with the numerical algorithms can be solved analytically, allowing for a direct analysis of the numerical solutions. The numerical approach permits us to gain an intuitive understanding of the methods and how they can be combined to improve the energy conserving properties of the algorithms. Following the approach by Neri[13] and Yoshida,[14,15] we illustrate how the symplectic structure of phase space is preserved by the symplectic algorithms and how higher order symplectic methods can be generated.

In Sec. II we briefly discuss linear symplectic structures and introduce the notion of a symplectic map. In Secs. III–V we discuss the symplectic Euler method and its adjoint, the velocity Verlet method, and a fourth-order method.

II. SYMPLECTIC FUNCTIONS AND ALGORITHMS

The setting for Hamiltonian mechanics is a $2n$-dimensional set of points with coordinates $(q,p)=(q_1,q_2,\ldots,q_n,p_1,p_2,\ldots,p_n)$. The dynamics is defined once a Hamiltonian function, $H(q,p)$, is specified. Each point of the set, called the phase space, represents a possible state of the system. As the system evolves from a given set of initial conditions, the associated states form a curve in phase space whose tangent vector at each point is $(H_p,-H_q)$. The identification of the tangent vector to the curve of states with the vector $(H_p,-H_q)$,

$$\frac{dq}{dt}=H_p,\quad \frac{dp}{dt}=-H_q, \tag{2.1}$$

is the geometric interpretation of Hamilton's equations.

We introduce the matrix $J=\left(\begin{smallmatrix}0 & I_n\\ -I_n & 0\end{smallmatrix}\right)$, set $z=(q,p)$, and write Hamilton's equations in the matrix form

$$\frac{d}{dt}z=J\nabla H(z). \tag{2.2}$$

Implicit in Hamilton's equations is a skew-symmetric, bilinear function of vectors, called the linear symplectic structure, defined as follows: For vectors $\mathbf{v}$ and $\mathbf{w}$, $[\mathbf{v},\mathbf{w}]=(J\mathbf{v},\mathbf{w})$, where $(,)$ is the usual Euclidean inner product. The symplectic structure has a simple geometric interpretation. For a system with N degrees of freedom, $[\mathbf{v},\mathbf{w}]$ is a sum of N terms. Each term represents an area. Each individual area is the projection of the parallelogram determined by $\mathbf{v}$ and $\mathbf{w}$ on its coordinate plane with coordinates (q_i,p_i). For a system with one degree of freedom, such as the harmonic oscillator, this sum of areas reduces to the area of a single parallelogram determined by $\mathbf{v}$ and $\mathbf{w}$. The geometry that results from the inclusion of such a linear symplectic structure on a $2n$-dimensional linear space is called a *symplectic geometry*.

When we solve Hamilton's equations with a given initial condition z_0, a function, $\varphi(t,z_0)$, called the phase flow, is

defined. This function defines the state of the system at time $t \geqslant 0$. Alternately, we can think of $\varphi(t,z_0)$ as a function, φ_t, that sends each point to the corresponding state at time t.

Henri Poincarè discovered that the phase flow has the following property. If $f'(z)$ denotes the Jacobian matrix of partial derivatives, $\partial f_i(z)/\partial z_j$, of the function $f(z) = f(z_1, z_2, \ldots, z_{2n}) = (f_1(z_1, z_2, \ldots, z_{2n}), f_2(z_1, z_2, \ldots, z_{2n}), \ldots, f_{2n}(z_1, z_2, \ldots, z_{2n}))$, the matrix $\varphi_t'(z)$ satisfies

$$[\varphi_t'(z)\mathbf{v}, \varphi_t'(z)\mathbf{w}] = [\mathbf{v}, \mathbf{w}], \tag{2.3}$$

for all vectors $\mathbf{v}$ and $\mathbf{w}$. Because applying the Jacobian matrix $\varphi_t'(z)$ to the vectors $\mathbf{v}$ and $\mathbf{w}$ generates a corresponding vector pair $\mathbf{v}_t$ and $\mathbf{w}_t$ at the later time t, Eq. (2.3) asserts that the sum of the areas of the projections remains constant in time. Thus, the phase flow preserves the linear symplectic structure. In general, a function f of phase space satisfies this condition if and only if

$$f'(z)^T J f'(z) = J. \tag{2.4}$$

If Eq. (2.4) holds, we call f *symplectic*.

For a given time step, Δt, a numerical algorithm $z_1 = A(\Delta t, z_0)$ can be thought of as a function on phase space. The algorithm is called symplectic if the function A is symplectic. Thus, symplectic algorithms share the same symplectic structure preserving property as the phase flows they approximate.

There are various ways that we can construct symplectic algorithms. One method[14,16–22] will be used in Secs. II–IV and depends on the following construction. By employing the Poisson bracket, we can rewrite the basic dynamical equation in a form that emphasizes the Lie algebraic structure that is implicit in symplectic geometry. For the functions f and g, the Poisson bracket, $\{f,g\}$, is defined by

$$\{f,g\} = \sum_{i=1}^{n} \frac{\partial f}{\partial q_i}\frac{\partial g}{\partial p_i} - \frac{\partial f}{\partial p_i}\frac{\partial g}{\partial q_i}. \tag{2.5}$$

The Poisson bracket is related to the symplectic structure as follows:

$$\{f,g\} = (J\nabla g, \nabla f) = [\nabla g, \nabla f]. \tag{2.6}$$

For a given function, H, we define the differential operator (the Liouville operator)

$$D_H f = \{f, H\}, \tag{2.7}$$

and use the same notation when f is a vector, with the understanding that in this case D_H acts on each component of f. Then Hamilton's equations may be written as

$$\frac{d}{dt} z(t) = D_H z(t), \tag{2.8}$$

which has the formal solution

$$z(t) = e^{tD_H} z(0), \tag{2.9}$$

providing the representation e^{tD_H} for the phase flow φ_t (for example, see Refs. 14 and 18 by Yoshida).

For Hamiltonian functions of the form

$$H(q,p) = V(q) + T(p), \tag{2.10}$$

the operator D_H takes the form

$$D_H = T'(p)\frac{\partial}{\partial q} - V'(q)\frac{\partial}{\partial p}. \tag{2.11}$$

If we apply Eq. (2.7), we see that

$$D_H z = \begin{pmatrix} T'(p) \\ -V'(q) \end{pmatrix} = J\nabla H(z). \tag{2.12}$$

For the harmonic oscillator with the Hamiltonian $H(q,p) = \frac{1}{2}(q^2+p^2)$, we have

$$\frac{d}{dt} z = D_H z = \begin{pmatrix} p \\ -q \end{pmatrix} = Jz, \tag{2.13}$$

which is a simple linear equation whose solution gives the phase flow:

$$e^{tD_H} = e^{tJ} = \begin{pmatrix} \cos(t) & \sin(t) \\ -\sin(t) & \cos(t) \end{pmatrix}. \tag{2.14}$$

III. FIRST-ORDER METHODS

As an introduction to symplectic algorithms, we begin with simple first-order methods. In general, a method is nth-order for a differential equation $y' = f(y)$, $y(t_0) = y_0$, if $y_1 - y(t_0 + \Delta t) = O(\Delta t^{n+1})$ as $\Delta t \to 0$, where y_1 is the result of applying the particular numerical method to the initial state y_0 for one time step. First-order methods are not likely to be used in any serious computation, but they provide a simple illustration of the differences between symplectic and nonsymplectic algorithms.

The most familiar of the first-order methods is the classic explicit Euler method:

$$q_{i+1} = q_i + p_i \Delta t, \tag{3.1a}$$

$$p_{i+1} = p_i + F_i \Delta t. \tag{3.1b}$$

This one-step algorithm does not conserve the total energy. For oscillatory systems such as the harmonic oscillator, the numerical solution that is obtained with this method diverges with each iteration from the true solution. In particular, the amplitude of the oscillations increases and the energy and the phase space area (see Fig. 1) increase monotonically with the same factor of $1+\Delta t^2$ for each iteration:

$$E_{i+1} = E_i(1 + \Delta t^2). \tag{3.2}$$

The implicit Euler method, given by

$$q_{i+1} = q_i + p_{i+1} \Delta t, \tag{3.3a}$$

$$p_{i+1} = p_i + F_{i+1} \Delta t, \tag{3.3b}$$

is comparable in error. With this method, the amplitude decreases, and the energy and area decrease by the same factor:

$$E_{i+1} = E_i \frac{1}{1 + \Delta t^2}. \tag{3.4}$$

For the harmonic oscillator, we find the $1+\Delta t^2$ factor associated with the Euler methods by expressing the equation of motion in terms of Hamilton's equations. The explicit Euler method is

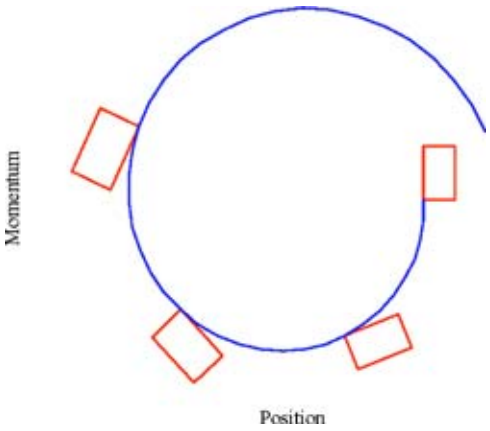

Fig. 1. A position-momentum phase plot using the explicit Euler method to determine the motion associated with the simple harmonic oscillator. The area in phase space increases by $1+\Delta t^2$ with each iteration as the phase trajectory spirals outward. The boxes provide an example of the growth of the area. The initial conditions in all the figures are a nonzero displacement ($q=0.2$) and a zero velocity ($p=0$).

$$\begin{pmatrix} q_{i+1} \\ p_{i+1} \end{pmatrix} = \begin{pmatrix} 1 & \Delta t \\ -\Delta t & 1 \end{pmatrix} \begin{pmatrix} q_i \\ p_i \end{pmatrix}, \tag{3.5}$$

which is the first-order approximation of the exact solution

$$\begin{pmatrix} q_{i+1} \\ p_{i+1} \end{pmatrix} = \begin{pmatrix} \cos(\Delta t) & \sin(\Delta t) \\ -\sin(\Delta t) & \cos(\Delta t) \end{pmatrix} \begin{pmatrix} q_i \\ p_i \end{pmatrix}. \tag{3.6}$$

A simple calculation shows that the explicit Euler method is not symplectic, because the test for symplecticity, Eq. (2.4), does not return J, but gives $(1+\Delta t^2)J$:

$$\begin{pmatrix} 1 & \Delta t \\ -\Delta t & 1 \end{pmatrix}^T \begin{pmatrix} 0 & 1 \\ -1 & 0 \end{pmatrix} \begin{pmatrix} 1 & \Delta t \\ -\Delta t & 1 \end{pmatrix} = \begin{pmatrix} 0 & 1+\Delta t^2 \\ -(1+\Delta t^2) & 0 \end{pmatrix}. \tag{3.7}$$

As demonstrated by Cromer,[15] a combination of explicit and implicit methods produces a symplectic method. If we write p in the implicit form and q in the explicit form (we could interchange the explicit and implicit roles—see the adjoint symplectic Euler method in the following), we have for any time-independent Hamiltonian $H(q,p)$,

$$q_{i+1} = q_i + \frac{\partial H(q_i, p_{i+1})}{\partial p} \Delta t, \tag{3.8a}$$

$$p_{i+1} = p_i - \frac{\partial H(q_i, p_{i+1})}{\partial q} \Delta t. \tag{3.8b}$$

For the harmonic oscillator, Eq. (3.8) becomes

$$q_{i+1} = q_i + p_{i+1} \Delta t, \tag{3.9a}$$

$$p_{i+1} = p_i - q_i \Delta t. \tag{3.9b}$$

Methods of this type are known as partitioned Euler methods.[16] To verify the assertion of symplecticity, we rewrite Eq. (3.9) by substituting for p_{i+1} in Eq. (3.9a) and obtain

$$\begin{pmatrix} q_{i+1} \\ p_{i+1} \end{pmatrix} = \begin{pmatrix} 1-\Delta t^2 & \Delta t \\ -\Delta t & 1 \end{pmatrix} \begin{pmatrix} q_i \\ p_i \end{pmatrix}. \tag{3.10}$$

We see that the algorithm is symplectic:

$$\begin{pmatrix} 1-\Delta t^2 & \Delta t \\ -\Delta t & 1 \end{pmatrix}^T \begin{pmatrix} 0 & 1 \\ -1 & 0 \end{pmatrix} \begin{pmatrix} 1-\Delta t^2 & \Delta t \\ -\Delta t & 1 \end{pmatrix} = \begin{pmatrix} 0 & 1 \\ -1 & 0 \end{pmatrix}. \tag{3.11}$$

We will refer to this method as the symplectic Euler method.

Partitioning in this way is an example of the *splitting method*,[17] where the differential equation of interest is divided into two, hopefully simpler, equations whose solutions can be combined into the solution of the original equation. For Hamiltonian systems with a separable Hamiltonian, $H(q,p)=T(p)+V(q)$, the equations of motion have the form

$$\begin{aligned} \frac{d}{dt} z(t) = D_H z(t) &= \begin{pmatrix} T'(p) \\ -V'(q) \end{pmatrix} \\ &= \begin{pmatrix} T'(p) \\ 0 \end{pmatrix} + \begin{pmatrix} 0 \\ -V'(q) \end{pmatrix} \\ &= D_T z(t) + D_V z(t). \end{aligned} \tag{3.12}$$

Equation (3.12) leads to the division

$$\frac{d}{dt} z(t) = D_T z(t) = \begin{pmatrix} T'(p) \\ 0 \end{pmatrix}, \tag{3.13a}$$

$$\frac{d}{dt} z(t) = D_V z(t) = \begin{pmatrix} 0 \\ -V'(q) \end{pmatrix}. \tag{3.13b}$$

Equation (3.13) is easily solved for a given initial state z_0. The solutions are given by the mappings

$$z(t) = \begin{pmatrix} q_0 + T'(p_0)t \\ p_0 \end{pmatrix} = e^{tD_T} z_0, \tag{3.14a}$$

$$z(t) = \begin{pmatrix} q_0 \\ p_0 - V'(q_0)t \end{pmatrix} = e^{tD_V} z_0. \tag{3.14b}$$

To construct the solution to Eq. (3.12), we evolve the state z_i by the second map, $z' = e^{\Delta t D_V} z_i$, and then evolve z' by the first map, and obtain

$$z_{i+1} = e^{\Delta t D_T} z' = e^{\Delta t D_T} e^{\Delta t D_V} z_i, \tag{3.15}$$

which is the symplectic Euler method. It is easy to check that Eq. (3.15) gives Eq. (3.10) for the harmonic oscillator.

Equation (2.9) shows that the exact solution to Hamilton's equations can be express in terms of the differential operator D_H. Because $D_H=D_T+D_V$ and the operators D_V and D_T do not commute, we know that[18]

$$e^{tD_H} = e^{t(D_T+D_V)} = e^{tD_T} e^{tD_V} + O(t^2). \tag{3.16}$$

Thus, the symplectic Euler method is a first-order method.

We can obtain a qualitative appreciation for the numerical behavior of the symplectic Euler method by examining it in more detail. We note that the q and p integrations are not in phase. One consequence is that as q increases, the potential energy peaks before the kinetic energy reaches its minimum, and the computed energy is greater than the true energy. As q decreases, the potential energy decreases before the comparable increase in the kinetic energy, and the computed energy is less than the true energy. When the motion is away from

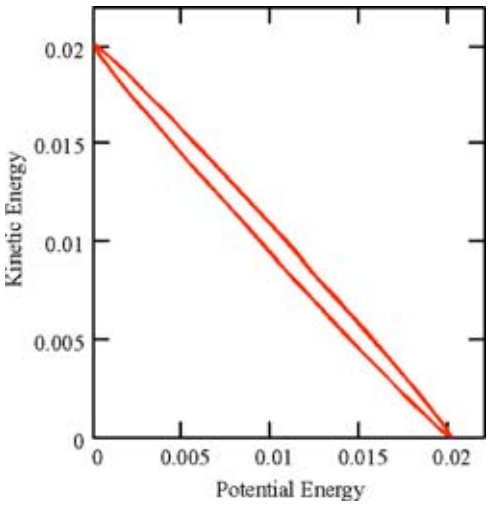

Fig. 2. A phase plot of the potential versus the kinetic energy as given by the numerical solution of the symplectic Euler method. The exact solution for the specific initial conditions used here would produce a straight line between the points (0.02,0) and (0,0.02). The elongated oval form is typical, and the general shape does not depend on the initial conditions.

the equilibrium position, there is excess energy; when the motion is toward equilibrium, there is an energy deficit. We observe these effects in the phase plot in Fig. 2 and the energy plots in Fig. 3.

The energy phase diagram in Fig. 2 shows approximately two orbits for each cycle. Ideally, the diagram should be a straight line between points where the energy is all kinetic or all potential. As the time step Δt is decreased, the phase difference decreases proportionally (as does the amplitude of the energy oscillation in Fig. 3), and the diagram more closely approaches the true solution.

Although the total energy is not conserved, the error has no secular increase, and the total energy remains near its true value. The magnitude of the computed energy oscillates asymmetrically at nearly twice the oscillator frequency about the true energy value with the amplitude of this oscillation related to the time step, as can be seen from the analytic description of the numerical solution given in the following. Although the local truncation error remains bounded, the problem associated with the accumulation of round-off errors remains.

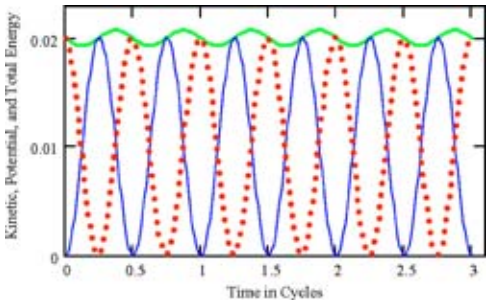

Fig. 3. The kinetic, potential, and total energy of the harmonic oscillator calculated using the symplectic Euler method. The computed total energy is the solid curve which oscillates about the analytic value of the total energy, in this case a constant of magnitude 0.02 J. The kinetic energy (solid) and potential energy (dotted) curves range from 0 to the approximate total energy.

The excursion of the total computed energy is not symmetric about the true energy and depends on the initial conditions. Further, the fact that the energy deviation of the numerical solution has very nearly twice the frequency of the oscillation suggests that there might exist a term in the computed energy proportional to qp, because this term would result in a product of sine and cosine terms providing the observed frequency doubling. That this is the case follows from the previous considerations, where it was observed that the symplectic Euler method is the result of the product of two simpler (and symplectic) transformations $e^{\Delta t D_V}$ and $e^{\Delta t D_T}$.

If we use the Baker-Campbell-Hausdorf formula,[4] a modified Hamiltonian function, H', can be found so that $e^{\Delta t D_T} e^{\Delta t D_V} = e^{\Delta t D_{H'}}$. We write

$$H'(q,p) = H_0 + \Delta t H_1 + \Delta t^2 H_2 + \cdots , \tag{3.17}$$

and use the Baker-Campbell-Hausdorf formula to determine H_k. For the harmonic oscillator, we find for H_0 and H_1

$$H_0 = T + V = \frac{1}{2}(q^2 + p^2). \tag{3.18a}$$

$$H_1 = -\frac{1}{2} T_p V_q = -\frac{pq}{2}. \tag{3.18b}$$

As higher-order terms in Δt are determined, we find that the expansion for H' takes the form

$$H'(q,p) = \Omega_1 (H_0(q,p) + H_1 \Delta t), \tag{3.19}$$

where $\Omega_1 = 1 + \Delta t^2/6 + \Delta t^4/30 + \cdots$. An analytic form for Ω_1 will be determined in the following. We see that to lowest order $H'(q,p) = H_0(z) + H_1(z)\Delta t$, which shows that the error in the energy in the symplectic Euler method is $O(\Delta t)$.

If we let $(q_{n+1}, p_{n+1}) = e^{\Delta t D_T} e^{\Delta t D_V}(q_n, p_n)$, it is easy to verify that

$$H'(q_{n+1}, p_{n+1}) = H'(q_n, p_n). \tag{3.20}$$

As Eq. (3.20) suggests, the numerical solution is the exact solution to the associated "modified" Hamiltonian system

$$\frac{dz(t)}{dt} = D_{H'} z(t). \tag{3.21}$$

Because H' is quadratic, this system is linear and can be solved exactly to yield the solutions

$$\begin{aligned} q'(t) &= q_0 \cos \omega_1 t + \frac{\Omega_1}{\omega_1}\left(\frac{\Delta t}{2} p_0 - q_0\right) \sin \omega_1 t, \\ p'(t) &= p_0 \cos \omega_1 t + \frac{\Omega_1}{\omega_1}\left(p_0 - \frac{\Delta t}{2} q_0\right) \sin \omega_1 t. \end{aligned} \tag{3.22}$$

Here (q_0, p_0) is the initial condition and $\omega_1 = \Omega_1 \sqrt{1 - \Delta t^2/4}$. To determine Ω_1, note that $(q'(\Delta t), p'(\Delta t)) = e^{\Delta t D_T} e^{\Delta t D_V}(q'(0), p'(0))$, which can be solved for Ω_1, yielding

$$\Omega_1 = \frac{\sin^{-1}(\Delta t \sqrt{1 - \Delta t^2/4})}{\Delta t \sqrt{1 - \Delta t^2/4}}, \tag{3.23}$$

so that the shift in frequency is $\omega_1 = 1 + O(\Delta t^2)$. We note that for small Δt, Ω_1 is well approximated by $3/(4\sqrt{1 - \Delta t^2/4} - 1)$. The dependence on Δt of the difference between the

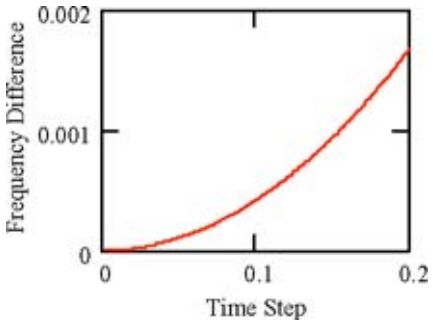

Fig. 4. The frequency shift as a function of the time step Δt.

shifted and the true frequency is shown in Fig. 4.

An analysis of the value of the energy of the numerical trajectory reveals that the average value of this energy may be greater or less than the true energy of the oscillator, depending on the initial conditions as is readily seen from

$$\langle H\rangle = \frac{1}{2}(q_0^2+p_0^2)\left(1+\frac{1}{4}\frac{\Delta t^2}{1-\Delta t^2/4}\right)-\frac{1}{2}\frac{\Delta t}{1-\Delta t^2/4}q_0p_0. \tag{3.24}$$

The average computed energy and the true energy are equal for

$$p_0=\frac{1}{\Delta t}[2\pm\sqrt{4-\Delta t^2}]q_0. \tag{3.25}$$

The lines for which these two energies are equal, scaled for emphasis (either multiplied or divided by Δt), separate what we call modified quadrants (see Fig. 5). The average value of the computed energy is less than the true energy in quadrants one and three and is greater in quadrants two and four. As $\Delta t\to 0$, the modified quadrants approach the true quadrants, and if we were to choose initial conditions at random, the likelihood that the average computed energy is greater or less than the true energy would become the same.

If we examine the initial conditions $q_0\neq 0$ and $p_0=0$ in the position-momentum phase diagram in Fig. 6, the phase difference in the q and p integrations mentioned previously is clearly visible in the asymmetry of the orbit; the qp term of Eq. (3.19) rotates the phase space ellipse. The corresponding energy deviation also is shown. An incomplete cycle is presented so that the evolution of the two curves can be followed.

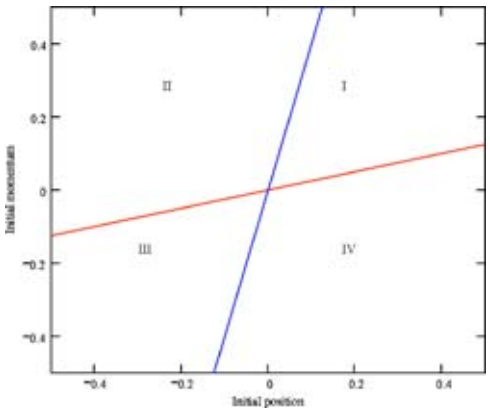

Fig. 5. The choice of the initial conditions determines whether the average value of the computed energy is greater than or less than the true energy. The two lines shown in the figure represent the equality of the true and the average computed energies and divide the plane into four modified quadrants. The average computed energy is greater than the true energy in quadrants two and four, and is less in quadrants one and three. The slopes of the two curves are scaled by factors of Δt and $1/\Delta t$.

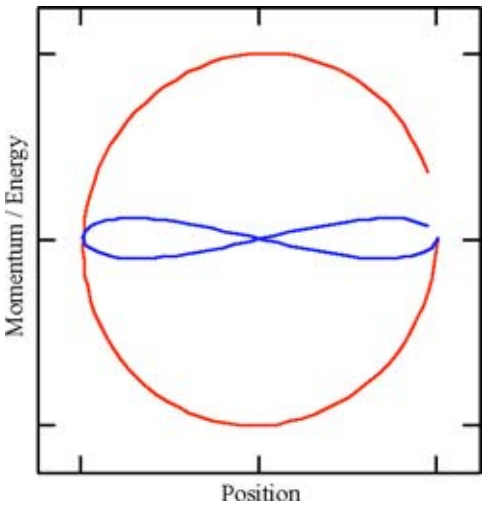

Fig. 6. The phase diagram for the position and momentum, together with the energy deviation from the true value (with two oscillations per cycle) versus position. The incomplete cycle permits us to follow the progress of the curves during the course of a cycle. The fact that the q and p calculations are not in phase is the source of the small but visible asymmetry.

There is a slight asymmetry in the phase diagram associated with the symplectic Euler method (Fig. 6). If we were to reflect this curve through the ordinate axis, the resulting phase diagram would look equally physical and suggests that there exists a similar but distinct algorithm that would yield essentially the same dynamic behavior, but with a phase difference. This reflection corresponds to an interchange of explicit and implicit roles for q and p in the algorithm. The resulting algorithm is the adjoint of the symplectic Euler method and is described in the following.

In Fig. 7 we show the kinetic, potential, and the total energy versus the position. The potential energy curve has the parabolic shape we would expect. The kinetic energy is not in phase with the position, and the kinetic energy oscillations show a phase difference of 2π divided by the number of iterations per cycle. If the abscissa were momentum instead of position, the kinetic and potential energy curves would interchange phase differences.

The symplectic Euler method is not the only first-order symplectic method. Because we expect that $D_{T+V}=D_{V+T}$, commuting the solution maps also should give an approximation to the exact solution map. The adjoint symplectic Euler method is the product

$$z_{i+1}=e^{\Delta t D_V}e^{\Delta t D_T}z_i, \tag{3.26}$$

which for the harmonic oscillator gives

$$\begin{pmatrix}q_{i+1}\\ p_{i+1}\end{pmatrix}=\begin{pmatrix}1 & \Delta t\\ -\Delta t & 1-\Delta t^2\end{pmatrix}\begin{pmatrix}q_i\\ p_i\end{pmatrix}. \tag{3.27}$$

The modified Hamiltonian of the adjoint method differs from Eq. (3.19) in that the $qp\Delta t/2$ term is added rather than subtracted. With this method we obtain a reflected phase diagram, analogous system behavior, and a similar curve for the

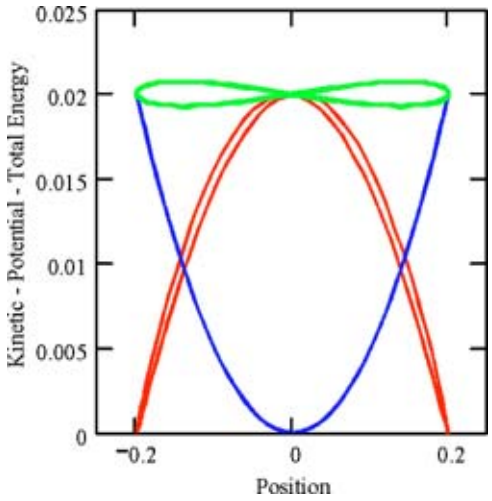

Fig. 7. The kinetic, potential, and total mechanical energy versus position. The lack of phase coherence between the position and momentum calculations, intrinsic to the first-order symplectic Euler method, is visible in the kinetic energy plot. If the abscissa had been the momentum, the phase difference would have appeared in the potential energy plot. Compare the oscillations in the total energy with those in Fig. 3. In Fig. 9 we present only the upper 1% of the energy range.

total energy except that it is out of phase with the energy curve obtained from the symplectic Euler method. Inspection of these two energy curves suggests that if we were to combine the two first-order methods, the energy deviation would be significantly reduced. A simple sum of the two total energy curves significantly reduces the energy variation to that of a second-order method. We will return to this point in Sec. IV.

IV. VELOCITY VERLET: A SECOND-ORDER SYMPLECTIC METHOD

The product of symplectic transformations also is symplectic. We can exploit this fact by combining the two symplectic Euler methods sequentially as the energy curves suggest. If we take two half-steps, using first one form and then its adjoint, we can combine the two half-step expressions into a single full-step expression. In terms of the exponential notation for the symplectic maps, this combination can be expressed as

$$(e^{(\Delta t/2)D_V}e^{(\Delta t/2)D_T})(e^{(\Delta t/2)D_T}e^{(\Delta t/2)D_V}) = e^{(\Delta t/2)D_V}e^{\Delta t D_T}e^{(\Delta t/2)D_V}. \tag{4.1}$$

For $T(p)=\frac{1}{2}p^2$, the resulting second-order algorithm can be expressed as

$$q_{i+1} = q_i + p_i\Delta t - \frac{1}{2}\frac{\partial V}{\partial q}(q_i)\Delta t^2,$$
$$p_{i+1} = p_i - \frac{1}{2}\left(\frac{\partial V}{\partial q}(q_i) + \frac{\partial V}{\partial q}(q_{i+1})\right)\Delta t, \tag{4.2}$$

which is the velocity form of the Verlet algorithm.[22,23]

In Fig. 8 the solid curve represents the path taken by two half-steps and shows the characteristic zig-zag of a split method; one half-step with the symplectic Euler method and the next half-step with its adjoint. The zig-zag curve provides

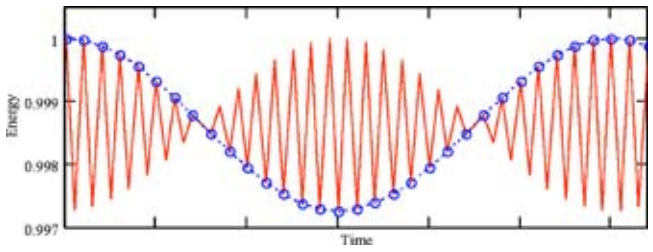

Fig. 8. Total energy curves, normalized by dividing by the analytic value of the energy, for the harmonic oscillator as determined by the symplectic Euler methods [Eqs. (3.9) and (3.27)] and the velocity Verlet method [open circles, Eq. (4.2)]. The jagged curve follows the symplectic Euler method for one-half step and then the adjoint method for a half-step.

a qualitative look at how the computation proceeds. The open circles are the results of the calculation using the velocity Verlet algorithm. In Fig. 8 the computed energy is normalized by dividing by the analytic value of the energy.

For a general Hamiltonian, the modified Hamiltonian for the Verlet algorithm is[4]

$$H'(z) = H_0(z) + \Delta t^2\left(\tfrac{1}{12}H_p^2(z)H_{qq}(z) - \tfrac{1}{24}H_q^2(z)H_{pp}(z)\right) + O(\Delta t^4). \tag{4.3}$$

As was the case for the first-order method, we can find an exact form for the modified Hamiltonian:

$$H'(q,p) = \Omega_2\left(\frac{1}{2}q^2 + \frac{1}{2}p^2 + \Delta t^2\left(\frac{1}{12}p^2 - \frac{1}{24}q^2\right) - \frac{\Delta t^4}{48}q^2\right), \tag{4.4}$$

from which exact solutions to the modified equations can be found by standard methods. The constant Ω_2 is found to satisfy

$$\Omega_2 = \frac{\sin^{-1}(\Delta t\sqrt{1-\Delta t^2/4})}{(1+\Delta t^2/6)\Delta t\sqrt{1-\Delta t^2/4}} = \frac{\Omega_1}{(1+\Delta t^2/6)}. \tag{4.5}$$

From the exact solutions we calculate that the average total energy of the numerical solution is given by

$$\langle H\rangle = \frac{1}{4}(q_0^2+p_0^2) + \frac{p_0^2}{4(1-\Delta t^2/4)} - \frac{q_0^2}{4}\left(1-\frac{\Delta t^2}{4}\right). \tag{4.6}$$

The frequency shift, $\omega_2=\Omega_1\sqrt{1-\Delta t^2/4}=\omega_1$, follows from the fact that the Verlet algorithm is a product of the symplectic Euler method and its adjoint.

The phase diagram of the kinetic versus the potential energy is a straight line with a slope of −0.996 in contrast to the first-order result in Fig. 2. The fact that the slope is less than −1 indicates that the kinetic energy is always less than the total energy.

V. FOURTH-ORDER METHODS

Higher-order methods tend to produce modified Hamiltonians that more closely approximate the original Hamiltonian. For example, for an nth-order symplectic method,[18]

$$H'(z) = H(z) + O(\Delta t^n). \tag{5.1}$$

As an example, we consider the fourth-order method of Candy and Rozmus (Fig. 9).[24] For each step in the integration, we calculate four substeps. For example, to integrate

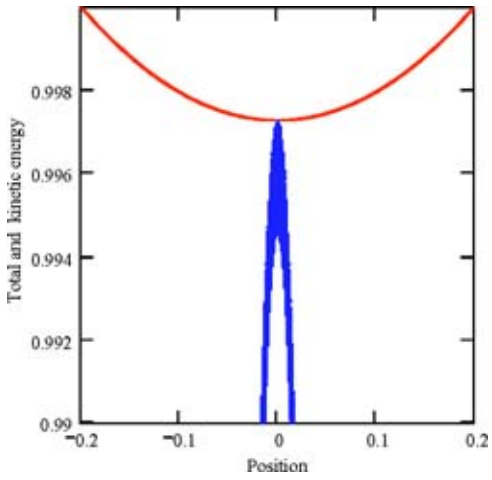

Fig. 9. The normalized total energy and the kinetic energy as computed by the velocity Verlet method are shown as a function of the position. The zero point is suppressed. Similar figures are obtained with higher order methods. With the fourth-order Candy-Rozmus method, the general shape is the same, but the energy variation is greatly reduced. Using optimal coefficients with the same algorithm, the energy variations are reduced still further, but the curvature of the total energy curve is reversed.

from (q_n,p_n) to (q_{n+1},p_{n+1}) we iterate the following pair of equations as i goes from 1 to 4

$$q_i = q_{i-1} + c_i p_i \Delta t, \qquad p_i = p_{i-1} - b_i V_q(q_{i-1})\Delta t', \tag{5.2}$$

where (q_1,p_1) takes on the values of (q_n,p_n) and the (q_4,p_4) values are assigned to (q_{n+1},p_{n+1}). The values for the fourth-order constants are[25]

$$b_1 = b_4 = \tfrac{1}{6}(2 + 2^{1/3} + 2^{-1/3}),$$
$$b_2 = b_3 = \tfrac{1}{6}(1 - 2^{1/3} - 2^{-1/3}), \tag{5.3}$$
$$c_1 = 0, \quad c_2 = c_4 = (2 - 2^{1/3})^{-1}, \quad c_3 = (1 - 2^{2/3})^{-1}.$$

If we write $S_i = e^{b_i \Delta t D_T} e^{c_i \Delta t D_V}$, the method of Candy and Rozmus[24] can be realized as a product of elementary exponential maps:[14]

$$z_{n+1} = S_4 S_3 S_2 S_1 z_n. \tag{5.4}$$

When applied to the harmonic oscillator, this fourth-order method gives more than two orders of magnitude improvement over the second-order methods in reducing the energy fluctuations.

Table I. Two sets of coefficients for the fourth-order method discussed in the text.

Order 4	Forest and Ruth (Ref. 24)	Optimal
b_1	$1/6(2+2^{1/3}+2^{-1/3})$	0.515 352 837 431 122 936 4
b_2	$1/6(1-2^{1/3}-2^{-1/3})$	−0.085 782 019 412 973 646
b_3	$1/6(1-2^{1/3}-2^{-1/3})$	0.441 583 023 616 466 524 2
b_4	$1/6(2+2^{1/3}+2^{-1/3})$	0.128 846 158 365 384 185 4
c_1	0	0.134 496 199 277 431 089 2
c_2	$(2-2^{1/3})^{-1}$	−0.224 819 803 079 420 805 8
c_3	$(1-2^{2/3})^{-1}$	0.756 320 000 515 668 291 1
c_4	$(2-2^{1/3})^{-1}$	0.334 003 603 286 321 425 5

Table II. Comparison of energy ranges for first-, second-, and fourth-order methods.

Method $\Delta t = 2\pi/60$	$\frac{E_{\max}-E_{\min}}{E_{\max}}$
Symplectic Euler	7.213×10^{-2}
Second-order velocity Verlet	2.742×10^{-3}
Fourth-order Candy and Rozmus (Ref. 24)	9.223×10^{-6}
Fourth-order optimal (Ref. 26)	1.123×10^{-7}

McLachlan and Atela[26] have constructed a fourth-order integrator where the optimal coefficients b_i, c_i were determined to minimize the time step error (see Table I). By using this integrator, the energy deviations as compared to those using the Candy-Rozmus coefficients are further reduced by almost two orders of magnitude.

A comparison of the energy deviations for the methods discussed for one step size is shown in Table I. In Table II we show a comparison of the energy deviation for the various methods. The energy deviation $(E_{\max}-E_{\min})E_{\max}$ is the same as the deviation of the slope in the potential energy versus kinetic energy phase diagram from the true value of −1. (We did not compute the slope for the Euler example as shown in Fig. 2.)

VI. COMMENTS

Symplectic methods offer distinct advantages over traditional Runge-Kutta methods in solving Hamilton's equations of motion because the symplectic structure of phase space is preserved by these methods, a feature shared by the flow map of the exact solution. Additionally, the trajectories produced by these algorithms remain on the surfaces of constant energy of the associated Hamiltonian function, so the energy of the system is closely approximated. Exactly solvable examples such as the harmonic oscillator reveal the structure of these algorithms, which can be developed from the symplectic structure inherent in phase space. The reader is invited to apply the symplectic Euler method to other Hamiltonian systems. The simple pendulum is treated by several authors (see, for example, Ref. 18). For a more challenging example, the reader can investigate the central force problem with $H(r,p_r,p_\theta)=(1/2m)(p_r^2+p_\theta^2/r^2)-k/r$, which can be perturbed by a term such as $-k_2/r^{3/2}$.

ACKNOWLEDGMENTS

The authors would like to acknowledge the help of anonymous reviewers, whose comments resulted in a greatly improved version of this paper.

[a]Electronic mail: donnelly@siena.edu
[b]Electronic mail: rogers@siena.edu

[1] Rene de Vogelaere, "Methods of integration which preserve the contact transformation property of the Hamiltonian equations," Report #4, Department of Mathematics, University of Notre Dame (1956).
[2] R. D. Ruth, "A canonical integration technique," IEEE Trans. Nucl. Sci. **NS-30**, 2669–2671 (1983).
[3] S. Edvardsson, K. G. Karlsson, and M. Engholm, "Accurate spin axes

and solar system dynamics: Climatic variations for the Earth and Mars," Astron. Astrophys. **384**, 689–701 (2002).
[4] H. Kinoshita, H. Yoshida, and H. Nakai, "Symplectic integrators and their application to dynamical astronomy," Celest. Mech. **50**, 59–71 (1991).
[5] S. Mikkola and P. Wiegert, "Regularizing time transformations in symplectic and composite integration," Celest. Mech. Dyn. Astron. **82**, 375–390 (2002).
[6] P. Saha and S. Tremaine, "Symplectic integrators for solar system dynamics," Astron. J. **104**, 1633–1640 (1992).
[7] J. Wisdom and M. Holman, "Symplectic maps for the n-body problem," Astron. J. **102**, 1528–1538 (1991).
[8] J. Wisdom and M. Holman, "Symplectic maps for the n-body problem: Stability analysis," Astron. J. **104**, 2022–2029 (1992).
[9] Robert D. Skeel, Guihua Zhang, and Tamar Schlick, "A family of symplectic integrators: Stability, accuracy, and molecular dynamics applications," SIAM J. Sci. Comput. (USA) **18**, 203–222 (1997).
[10] Peter Nettesheim, Folkmar A. Bornemann, Burkhard Schmidt, and Christof Schütte, "An explicit and symplectic integrator for quantum-classical molecular dynamics," Chem. Phys. Lett. **256**, 581–588 (1996).
[11] Peter Nettesheim and Sebastian Reich, "Symplectic multiple-time-stepping integrators for quantum-classical molecular dynamics," in *Computational Molecular Dynamics: Challenges, Methods, Ideas*, edited by P. Deuflhard, J. Hermans, B. Leimkuhler, A. E. Mark, S. Reich, and R. D. Skeel (Springer, New York, 1998), pp. 412–420.
[12] Andreas Dullweber, Benedict Leimkuhlera, and Robert McLachlan, "Symplectic splitting methods for rigid body molecular dynamics," J. Chem. Phys. **107**, 5840–5851 (1997).
[13] F. Neri, "Lie algebras and canonical integration," Technical Report, Department of Physics, University of Maryland, preprint (1987), unpublished.
[14] Haruo Yoshida, "Construction of higher order symplectic integrators," Phys. Lett. A **150**, 262–268 (1990).
[15] This method has been found more than once. See, for example, "Stable solutions using the Euler approximation." Alan Cromer, Am. J. Phys. **49**, 455–459 (1981).
[16] E. Harier, C. Lubich, and G. Wanner, *Geometric Numerical Integration, Structure-Preserving Algorithms for Ordinary Differential Equations* (Springer, New York, 2002).
[17] Haruo Yoshida, "Symplectic integrators for Hamiltonian systems: Basic theory," in *Chaos, Resonance, and Collective Dynamical Phenomena in the Solar System*, Proceedings of the 152nd Symposium of the International Astronomical Union (1991), p. 407.
[18] Haruo Yoshida, "Recent progress in the theory and application of symplectic integrators," Celest. Mech. Dyn. Astron. **56**, 27–43 (1993).
[19] J. M. Sanz-Serna, "Symplectic integrators for Hamiltonian problems: An overview," Acta Numerica **1**, 243–286 (1992).
[20] V. I. Arnold, *Mathematical Methods of Classical Mechanics* (Springer-Verlag, New York, 1978).
[21] B. A. Shadwick, Walter F. Buell, and John C. Bowman, "Structure preserving integration algorithms," in *Scientific Computing and Applications* (Nova Science, Commack, New York, 2001), Vol. 7, pp. 247–255.
[22] Loup Verlet, "Computer 'experiments' on classical fluids. I. Thermodynamical properties of Lennard-Jones molecules," Phys. Rev. **159**, 98–103 (1967).
[23] See, for example, H. Gould and J. Tobochnik, *An Introduction to Computer Simulation Methods*, 2nd ed. (Addison-Wesley, Reading, MA, 1996), p. 123.
[24] J. Candy and W. Rozmus, "A symplectic integration algorithm for separable Hamiltonian functions," J. Comput. Phys. **92**, 230–256 (1991).
[25] Franz J. Vesely, *Computational Physics: An Introduction*, 2nd ed. (Kluwer Academic, New York, 2001).
[26] R. I. McLachlan, "The accuracy of symplectic integrators," Nonlinearity **5**, 541–562 (1992).